

Electric Field Analysis and Shielding Optimization of 15kV DC Switchgear Wall Bushing

Chengkun Zhang ^{1, a}, Rui An ^{1, b}, Chao Yang ^{1, c}, Zhe Li ^{1, d}, and Lun Huang ^{1, e}

¹ XD Baoji Electric Co., Ltd, Shaanxi Baoji 721000, CHINA.

^a ckzhang9527@163.com, ^b anruiook@163.com, ^c 247591745@163.com, ^d lizhe@xdbjdq.com,

^e huanglun@xdbjdq.com

Abstract. Aiming at the 15kV direct current (DC) switchgear busbar wall bushing is prone to local aging resulting in insufficient insulation capacity. In this paper, according to the response surface parameter optimisation method, Maxwell-Workbench joint simulation is established to carry out numerical calculations of electric field on the parameterised model of shielding ring of wall bushing, and to study the influence of the structural parameters of the shielding ring on the distribution of electric field and the optimal combination of structural parameters of the shielding ring. The results show that the maximum electric field intensity without the shielding ring appears at the position of the connection between the fixing plate and the wall bushing and at the position where the inside diameter of the casing is closest to the busbar. The high potential shielding ring mainly affects the electric field strength of the air region inside the wall bushing, and the ground potential shielding ring mainly affects the electric field strength of the air region outside the wall bushing; The ground potential shielding ring should be as far as possible beyond the location where the fixing plate is connected to the wall bushing; The high ground potential shielding ring is closer, the electric field between the shielding rings is drum-shaped, and the electric field strength inside the casing is higher; The high ground voltage shielding ring is farther away, the electric field is funnel-shaped, and the electric field intensity is small at the connection position between the wall bushing and the fixing plate, which is favourable to the insulation life of the wall bushing and the partial discharge; Analysing and obtaining 4 groups of shielding ring structure parameter combinations that meet the insulation requirements can effectively improve the electric field distribution and reduce the electric field intensity.

Keywords: Wall Bushing, Shielding Ring, Maxwell-Workbench, Electric field simulation.

1. Introduction

DC metal-enclosed switchgear and control equipment, in the DC system bears the role of receiving, feeding and protection, and plays a key role in the safe production and reliable operation of DC power grid [1-2]. Wall bushing as a key device to isolate the busbar and the switchgear body, to ensure good insulation, with a safe insulation margin, are directly affecting the normal operation of the switchgear [3-4]. In order to ensure the safe and stable operation of the switchgear cabinet, the main method to improve the insulation performance of the wall bushing is to install shielding rings, and research on the number of shielding rings, installation dimensions, structural dimensions and other parameters, however, the experimental research exists in the waste of materials, the cycle time is long, and the safety of the low problems [5-7]. With the continuous improvement of computer-aided engineering and computer arithmetic, simulation replaces the preliminary experimental study by firstly designing the structural parameters, then solving the eligible parameter combinations through simulation, and finally carrying out the experimental verification, which reduces the cost, saves time, and ensures the reliability of the product [8-9].

Han et al [10] used Ansys Workbench software for the electric field of wall bushing, proposed the use of a single ground potential shielding ring or a combination of high potential and ground potential shielding ring to solve the problem of local electric field concentration in the wall bushing, and analysed the dimensions of the high and ground potential shielding ring as well as the effect of dimensional changes on the distribution of electric field in the wall bushing. Deng et al [11] used the finite element analysis software ANSYS Workbench to simulate the wall bushing without

shielding, with high and low potential shielding, and optimised high and low potential shielding of the three schemes, respectively, and the optimised wall bushing internal air region and the external air region of the electric field are lower than the air critical breakdown field strength value.

In this paper, the wall bushing used in 15kV hybrid MV DC switchgear is selected for research. The joint simulation method of Maxwell and Workbench is adopted. Firstly, a two-dimensional parametric model of wall bushing is established in Maxwell software, and then multivariate parameter and output variable settings are completed; secondly, according to the response surface parameter optimization method, the parameter solution range and criterion are set up in the joint Workbench platform, and numerical calculations are carried out, and the structural parameter combinations of wall bushing that satisfy the conditions are obtained at the end. The structural parameter combinations of wall bushing are calculated to meet the conditions. The electric field distribution in the inside and outside air regions of the wall bushing without shielding ring is studied; the influence of different parameters on the inside and outside air regions and the internal electric field strength of the wall bushing is analysed; and the structural parameter combinations of the shielding ring of the wall bushing for the 15kV hybrid MV DC switchgear are obtained to satisfy the conditions, which provides a method for the design of the subsequent shielding ring of the wall bushing.

2. Numerical Modelling

2.1 Parametric Modelling of Bulkhead Sleeves

In order to reduce the calculation cost and improve the calculation efficiency, the parametric two-dimensional model of wall bushing is established in Maxwell software, as shown in Fig. 1, which lays the foundation for the subsequent further calculation.

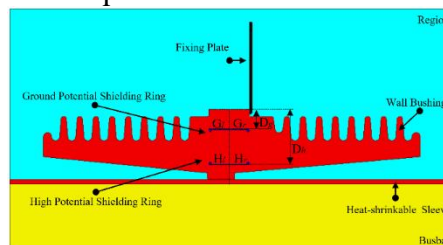


Fig. 1 Parametric model of 2D wall bushing

As can be seen from Fig. 1, the 2D wall bushing parametric model consists of wall bushing body, wall bushing fixing plate, busbar, heat-shrinkable casing, high potential shielding ring and low potential shielding ring. Among them, Gr indicates the distance between the ground potential shielding ring and the right installation position of the casing, Gl indicates the distance between the ground potential shielding ring and the left installation position of the casing, Hr indicates the distance between the high potential shielding ring and the right installation position of the casing, Hl indicates the distance between the high potential shielding ring and the left installation position of the casing, Dh indicates the distance between the high potential shielding ring and the top installation position of the casing, and Dg indicates the distance between the ground potential shielding ring and the top installation position of the casing.

2.2 Material Properties

The material properties of the 2D wall bushing parametric model are shown in Table 1 [12].

Table 1. Material properties

Name of Model	Name of Material	Relative Permittivity	Bulk Conductivity s/m
Busbar	Copper	1.0	5.8E7
Heat-shrinkable Sleeve	PVC	4.6	1E-15
Wall Bushing	Epoxy Resin	3.4	1E-13

Shielding Rings	Aluminium Sheet	1.0	3.77E+07
Fixing Plate	Aluminium Zinc Clad Plate	1.0	1.1E+06
Region	Air	1.0	2.6E-17

2.3 Simulation Programmes

The numerical solution scheme of the two-dimensional wall bushing parametric model is shown in Fig. 2.

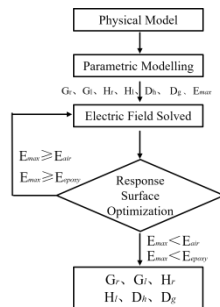


Table 2. Shield ring parameter ranges

Parametric	Range/mm
G_r	0-35
G_l	0-5
H_r	0-50
H_l	0-50
D_h	7-25
D_g	29-39

Fig. 2 Simulation programme

Firstly, the 2D wall bushing parametric model is established in Maxwell software. Secondly, set up the electrostatic field solution, select the default boundary conditions, select the DC voltage source for excitation, the voltage value is 105kV, the mesh defaults to the second-order mesh, the allowable solution error is 1%, and set up the output variable of the maximum electric field strength E_{max} ; Secondly, call the Workbench platform to solve the two-dimensional wall bushing parametric model. Thirdly, call the response surface analysis module in the Workbench platform, set the range of variation of the shielding ring structure parameters, as shown in Table 2, the maximum electric field strength of the air is taken as $2.95E6$ v/m, and the maximum electric field strength of the epoxy resin is taken as $2.95E7$ v/m [12]. Finally, the optimal structural parameter combinations are obtained by the joint solution of the response surface analysis module.

3. Results and Discussion

The ground potential shielding ring connects to the fixing plate and the high potential shielding ring connects to the busbar, creating a uniform potential difference inside the wall bushing. Wall bushing is made of epoxy resin composite material, its insulation strength is greater than the air insulation strength ($3E7$ v/m), effectively avoiding internal breakdown. The air region outside the wall bushing is kept at a low level of electric field strength by the shielding ring to avoid air breakdown and improve the overall insulation performance of the wall bushing. In this section, simulation calculations are first carried out for the casing without shielding ring to analyse the internal and external electric field distribution of the wall bushing.

3.1 Without Shielding Ring

The results of the numerical analysis of the electric field strength of the wall bushing without the shielding ring are shown in Fig. 3.

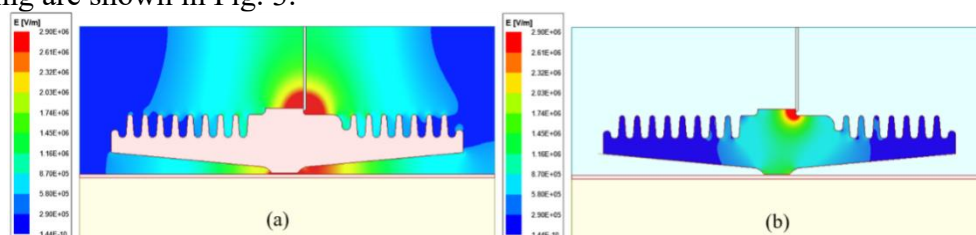


Fig. 3 Distribution of electric field in wall bushing without shielding ring installed
As can be seen from Fig. 3, (a) represents the cloud diagram of electric field strength distribution

in the air region of the wall bushing, the maximum value of electric field strength in the outside air region is at the position where the fixing plate is connected to the wall bushing ($1.01\text{E}6\text{v/m}$), and the maximum value of electric field strength in the inside air region is at the nearest position of the busbar and the wall bushing ($6.17\text{E}6\text{v/m}$). (b) represents the cloud diagram of the distribution of electric field strength inside the wall bushing, and the maximum value of electric field strength is at the position of the fixed plate mounting ($1.37\text{E}7\text{ v/m}$), although it does not exceed the maximum electric field strength of epoxy resin ($2.95\text{ E}7\text{ v/m}$), but partial discharges are prone to occur here, and the insulating capacity of the wall bushing gradually decreases with time, and the risk of the busbar discharging to the switchgear increases, and a charged operation process major accidents may occur. Therefore, under the premise of guaranteeing that the air outside the wall bushing does not break through during the design process, consideration should also be given to reducing the concentration of the electric field inside the wall bushing in order to improve the overall insulating performance.

3.2 Shielding Ring

The control variable method is used to calculate the electric field distribution in the air region of the wall bushing under different combinations of structural parameters, and the change curve of the maximum electric field intensity in the air region at different structural parameters is plotted to analyse the influence of structural parameters on the electric field distribution, as shown in Fig. 4.

As can be seen from Fig. 4(a), the air region electric field strength inside the wall bushing shows a decreasing trend when H_I increases with constant G_r , H_r , D_g and D_h parameters, and the air region electric field strength inside the wall bushing shows an increasing trend and the electric field strengths are all less than the air insulation strength when G_I increases.

As can be seen from Fig. 4(d), when both H_I and G_I are increased, the electric field strength in the air region outside the wall bushing shows an increasing trend and the electric field strength exceeds the air insulation strength ($2.95\text{E}6\text{ v/m}$). In order to study the effect of parameters H_I and G_I on the electric field distribution, the electric field distribution is analysed for H_I of 5mm, 20mm, 35mm and G_I of 1mm, 3mm and 5mm as shown in Fig. 5.

As can be seen from Fig. 5(a) (c), the centre region of the inside surface of the wall bushing is close to the busbar, and the electric field concentration in the inside air region is obvious ($6.61\text{E}6\text{ v/m}$), and the equipotential region formed between the high-potential shielding ring and the busbar can effectively reduce the effect of electric field concentration ($8.60\text{E}5\text{ v/m}$). The electric field intensity in the area not covered by the high potential shielding ring decreases significantly ($3.27\text{E}6\text{ v/m}$), H_I increases and the equipotential region expands to the left, and the electric field intensity in the inside air region of the wall bushing decreases ($6.61\text{E}6\text{-}6.20\text{E}5\text{ v/m}$).

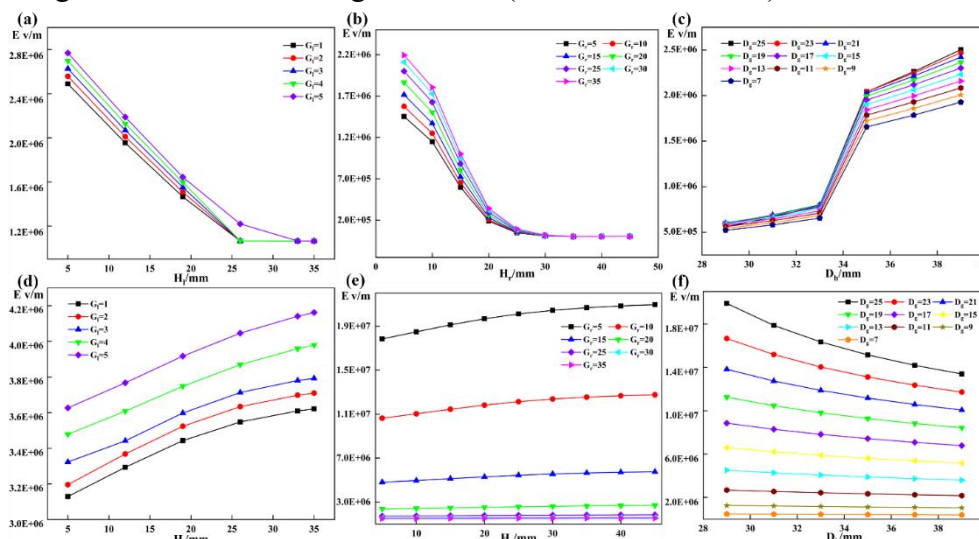


Fig. 4 Variation curve of maximum electric field strength in air region of wall bushing.(a) (b) (c)

indicates the air region inside the wall bushing, and (d) (e) (f) indicates the air region outside the wall bushing.

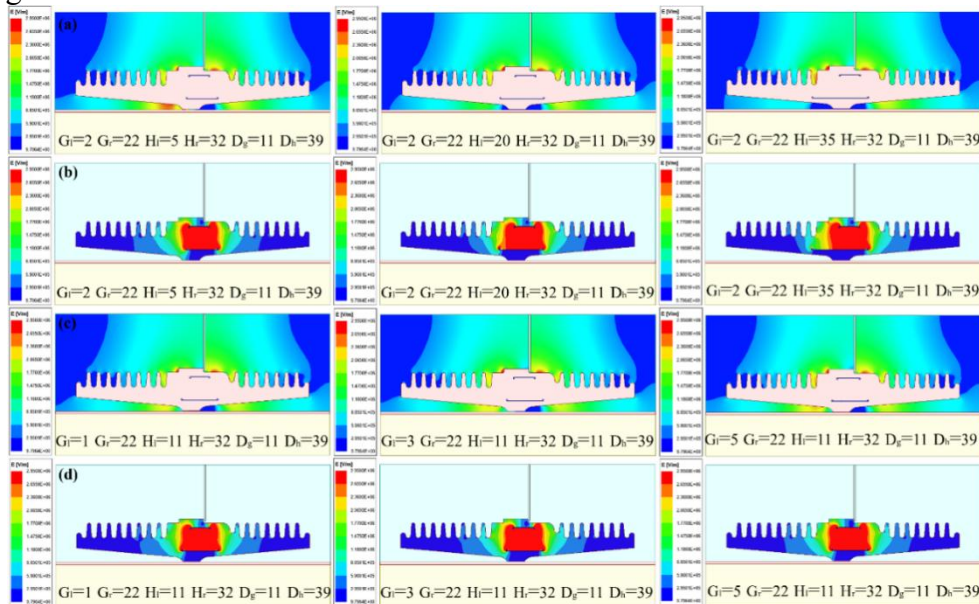


Fig. 5 Electric field distribution. (a) represents the air region electric field distribution when parameter Hl is varied, (b) represents the electric field distribution inside the wall bushing when parameter Hl is varied, (c) represents the air region electric field distribution when parameter Gl is varied, and (d) represents the electric field distribution inside the wall bushing when parameter Gl is varied.

As can be seen from Fig. 5(b) (d), the electric field is formed between the high potential shielding rings inside the wall bushing ($4.1E6$ v/m), and when the ground potential shielding ring Gl increases, the electric field region also expands to the left, and the strength of the electric field in the outside air region of the wall bushing rises ($2.91E6$ - $3.37E6$ v/m). So it is worth noting that the effect of parameter Hl is greater than Gl for the inside air region of the wall bushing, on the contrary for the outside air region of the wall bushing, the effect of parameter Hl is less than Gl.

As can be seen from Fig. 3(c), the parameters Gl, Hl, Dg and Dh are unchanged, and when Hr increases, the air region electric field strength inside the wall bushing decreases, and the electric field strengths are all smaller than the air insulating strengths, and the reason for the change is the same as that of the parameter Hl.

As can be seen from Fig. 3(d), the parameter Hr increases, the air region electric field strength outside the wall bushing increases, the parameter Gr increases, the air region electric field strength outside the wall bushing decreases, and when the parameter Gr is less than 20 mm, the air region electric field strength is greater than the air insulation strength.

In order to study the effect of parameters Hr and Gr on the electric field distribution, the electric field distribution is analysed for Gr of 5mm, 20mm and 35mm as shown in Fig. 6.

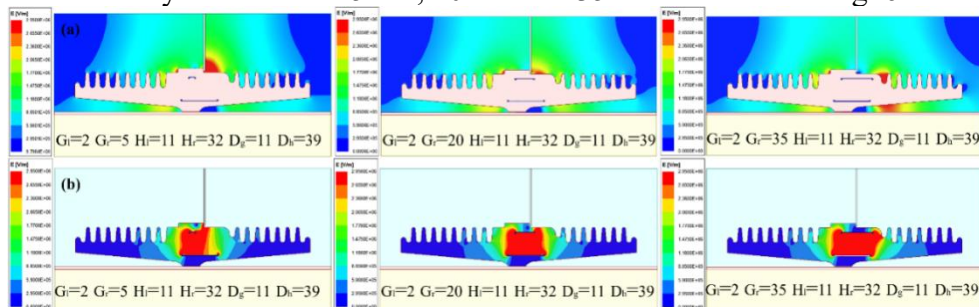


Fig. 6 Electric field distribution. (a) represents the air region electric field distribution when parameter Gr is varied, (b) represents the electric field distribution inside the wall bushing when

parameter G_r is varied.

As can be seen in Fig. 6, when the parameter G_r is 5mm, the electric field strength at the connection between the fixing plate and the wall bushing exceeds the air insulation strength ($1.14E7$ v/m), when the parameter G_r is 20mm, the electric field strength at the connection position is significantly reduced ($9.25E5$ v/m), when the parameter G_r is 35mm, the electric field strength at the connection position continues to be reduced ($2.12E5$ v/m), but due to the shift of the electric field region to the right, the electric field in the air region outside the wall bushing is elevated ($4.85E6$ v/m). By analysing and comparing it is not difficult to find that the parameter G_r and G_l change rule is consistent, ground potential shielding ring in the design process should try to exceed the fixing plate and wall bushing connection position, but should not be too large.

As can be seen in Fig. 3(e), the parameters G_r , H_r , G_l and H_l parameters are constant, the air region electric field strength inside the wall bushing decreases as the parameter D_h increases, and the air region electric field strength inside the wall bushing increases as the parameter D_g increases, and the electric field strengths are all less than the air insulation strength.

As can be seen in Fig. 3(f), the electric field strength of the air region outside the wall bushing increases with the increase of parameter D_g and decreases with the increase of parameter D_h . Parameter D_g in the range of 13-25 mm, the external air region electric field strength exceeds the air insulation level.

In order to study the effect of parameters D_g and D_h on the electric field distribution, the electric field distribution is analysed for D_g of 7mm, 17mm, 25mm and D_h of 29mm, 34mm and 39mm as shown in Fig. 7.

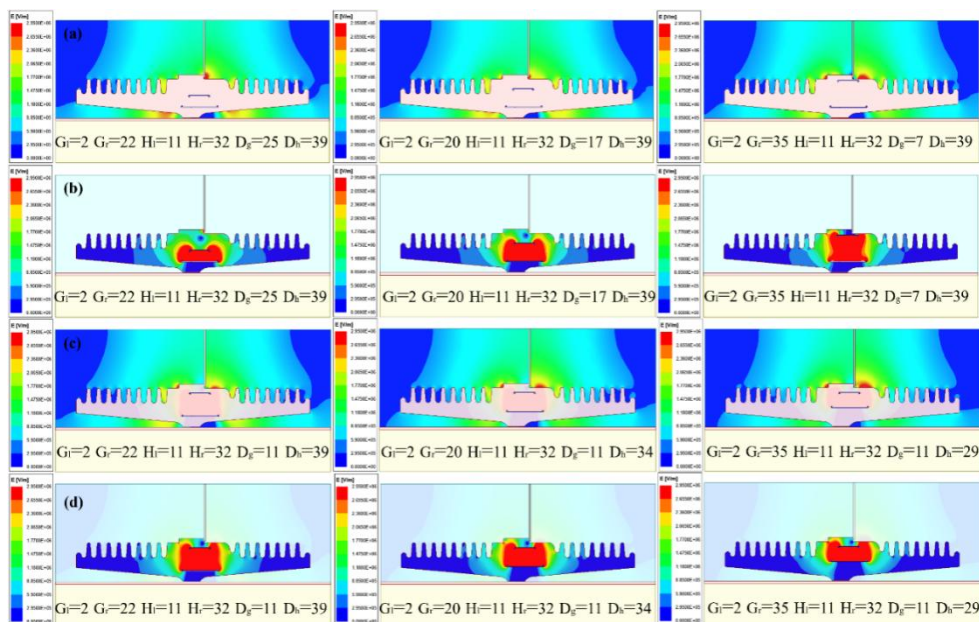


Fig. 7 Electric field distribution. (a) represents the air region electric field distribution when parameter D_g is varied, (b) represents the electric field distribution inside the wall bushing when parameter D_g is varied, (c) represents the air region electric field distribution when parameter D_h is varied, and (d) represents the electric field distribution inside the wall bushing when parameter D_h is varied.

As can be seen in Fig. 7, when the distance between the shielding rings of the high ground voltage is small ($25 > D_g > 13$, $29 < D_h < 35$), the electric field between the shielding rings is in the form of a bulge, and the electric field gathers in a smaller area, and the strength of the electric field inside the wall bushing is larger ($7.79E6$ v/m), and on the one hand, the electric field at both ends of the shielding rings radiates outward, the strength of the electric field in the air region of the wall bushing is elevated, and the possibility of air breakdown is elevated, especially at the The connection position of the wall bushing to the fixing plate ($5.19E6$ v/m), on the other hand, is

unfavourable to the working life of the wall bushing. When the distance between the shielding rings of the high ground voltage is larger ($7 \leq D_g \leq 13$, $39 \geq D_h \geq 35$), the electric field distribution between the shielding rings is funnel-shaped, the electric field strength inside the wall bushing decreases ($3.0E6$ v/m) and stays low, and the electric field strength of the connection position between the wall bushing and the fixing plate is lower than the air insulation strength ($2.65E6$ v/m), which is not favourable to the working life of the wall bushing and partial discharge is favourable.

3.3 Shield Ring Optimization Parameters

The influence of shielding ring parameters on the electric field distribution is studied by the control variable method. In this section, the optimal structural parameter combinations of the shielding ring to satisfy the electric field insulation strength requirements are solved by using the response surface optimization method, and the results are shown in Table 3.

Table 3. Parameter combination schemes

Scheme	G_l	G_r	H_l	H_r	D_g	D_h
1	2	22	11	32	11	39
2	1	24	14	21	9	38
3	3	26	19	34	11	35
4	4	25	22	39	13	39

The electric field distribution for parameter combination scheme 1 is shown in Fig. 8.

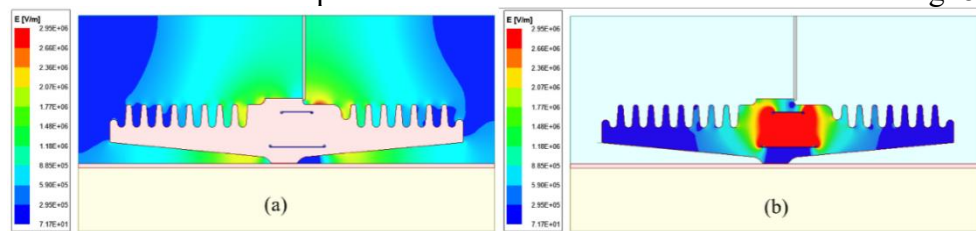


Fig. 8 electric field distribution for Scheme 1

As can be seen from Fig. 8, the maximum electric field strength in the external air region of the wall bushing with the parameters shown in Scheme 1 is $2.94E6$ v/m, the maximum electric field strength in the internal air region is $1.87E6$ v/m, and the maximum electric field strength in the internal part of the wall bushing is $3.72E6$ v/m, which meets the requirements for insulation strength.

4. Conclusion

(1). The method of Maxwell-Workbench joint simulation to solve the structural parameters of the shielding ring and get the optimal combination of structural parameters is feasible.

(2). The high potential shielding ring mainly affects the intensity of electric field in the air region inside the wall casing, the ground potential shielding ring mainly affects the intensity of electric field in the air region outside the wall casing, the ground potential shielding ring should try to exceed the position of connection between the fixing plate and the wall casing, but it should not be too large.

(3). High ground potential shielding ring distance is closer, the electric field between the shielding ring is drum-shaped, through the wall casing internal electric field intensity is large, through the wall casing and fixing plate connection location by its influence on the possibility of air breakdown increases, is not conducive to through the wall casing insulation life. On the contrary, the high potential shielding ring is farther away, the electric field between the shielding ring is funnel-shaped, the electric field strength of the connection position between the wall bushing and the fixing plate is small, which is favorable to the working life of the wall bushing and the partial discharge.

5. Acknowledgements

This research was financially supported by XD Baoji Electric Co., Ltd Project of China (NO. X24-0214, X24-0304).

References

- [1] WANG Yuhong, FU Yuntao, ZENG Qi, SONG Yuyan. Review on Key Techniques for Fault Protection of Flexible DC Grids [J]. High Voltage Engineering, 2019 (8): 2362-2374.
- [2] LI Xingyuan, ZENG Qi, WANG Yuhong, ZHANG Yingmin. Control Strategies of Voltage Source Converter Based Direct Current Transmission System [J]. High Voltage Engineering, 2016, 42(10): 3025-3037.
- [3] ZHANG Hou, HAN Xingjun, GUO Anqi, SHI Jiahao, ZHENG Hong. Analysis of insulation breakdown of the wall bushing in a flexible DC converter station and modification mechanism research on the material [J]. Zhejiang Electric Power, 2023, 42(5).
- [4] PAN Yiwei, CHEN Jiansheng, LIN Jian, JIN Jiamin. Cause Analysis and Treatment on Discharging of 40.5 kV Switch Cabinet [J]. Zhejiang Electric Power, 2014(3): 35-37.
- [5] WANG Haiyan, ZHU Zhihao, FEI Xiang, ZHU Yanqing, YUAN Duanlei. Electric Field Optimization and Structure Design of Wall Bushing in 40.5 kV Air-insulated Switchgear [J]. High Voltage Apparatus, 2019, 55(01): 59-63.
- [6] JIA Yongyong, YANG Jinggang, GAO Shan, TAO Fengbo, ZOU Hai, ZHANG Guogang. Simulation of Internal Electric Field of High-voltage Metal-enclosed Switchgear and Influencing Factors [J]. High Voltage Apparatus, 2017, 53(06): 154-160.
- [7] TAN Dongxian, HE Yiling, LIN Jun, MAO Lei, LIU Yuhua, XIAO Dengming. Investigations on Insulation Characteristics of 12 kV Composite Insulated Switchgear [J]. High Voltage Apparatus, 2018, 54(04): 28-33.
- [8] HUANG Jingjing, CHONG Jiali. Electric Field Simulation and Structure Optimization for Wall Bushing of KYN61-40.5 kV Switchgear [J]. High Voltage Apparatus, 2021, 57(01): 68-74.
- [9] Lang F, Zhang H. Fault analysis and structure optimization of 40.5 kV wall bushing [C], 2015 5th International Conference on Electric Utility Deregulation and Restructuring and Power Technologies (DRPT). IEEE, 2015: 1628-1631.
- [10] HAN Shaigen, CAO Bin, HUANG Qiang, MA Zongxiong. Electric Field Analysis and Shielding Optimization of 40.5 kV Wall Bushing [J]. High Voltage Apparatus, 2017, 53(01): 113-118.
- [11] DENG Hu, PENG Yan-ying, YOU Yi-min, MA Zong-xiong, XIAO Liang-xian. Simulation and Design Optimization of the Shielding Wall Bushing [J]. Journal of Kiamen University of Technology, 2015(5): 41-45.
- [12] Li C L, Liu R, Li P H, et al. Electric field simulation of typical defects in the epoxy/paper composites insulated tubular bus [C], Materials Science Forum. Trans Tech Publications Ltd, 2018, 922: 157-162.